Tech Memo
P 1204

Tech Memo
P 1204

ROYAL AEROSPACE ESTABLISHMENT

Technical Memorandum

February 1991

Application of S1BYL2 to the AGARD WG18 Compressor Test Cases

by

W. J. Calvert

Procurement Executive, Ministry of Defence
Farnborough, Hampshire

UNLIMITED

CONDITIONS OF RELEASE

0099152 301533

********** DRIC U

********** DRIC Y

Reports quoted are not necessarily available to members of the public or to commercial organisations.

ROYAL AEROSPACE ESTABLISHMENT

Technical Memorandum P 1204

Received for printing 27 February 1991

APPLICATION OF SIBYL2 TO THE AGARD WG18 COMPRESSOR TEST CASES

by

W. J. Calvert

SUMMARY

SIBYL2 is an inviscid-viscous blade-to-blade method for calculating the detailed aerodynamics and overall performance of compressor blades. It may be applied either on its own to predict the flow for individual blade sections, such as the mid span of a linear cascade, or in conjunction with a throughflow calculation to predict the performance of a complete axial compressor.

A previous AGARD paper by the author described applications of SIBYL2 to most of the compressor cascade test cases which have subsequently been selected by AGARD Working Group 18: generally good agreement was obtained. This current paper presents new predictions for the V2 and ARL SL19 cascades and for the high speed compressor cases. It is hoped that this will be one of many sets of calculations for these cases, so that an improved understanding of each case may be obtained, together with an appreciation of the strengths and weaknesses of different computational approaches.

This Memorandum is a facsimile of a paper prepared for the 77th Symposium of the AGARD Propulsion and Energetics Panel on "CFD Techniques for Propulsion Applications" to be held in San Antonio, Texas, USA, 27-31 May, 1991.

LIST OF CONTENTS

W J Calvert
Propulsion Department
Royal Aerospace Establishment
Pyestock, Farnborough,
Hampshire, UK

SUMMARY

S1BYL2 is an inviscid-viscous blade-to-blade method for calculating the detailed aerodynamics and overall performance of compressor blades. It may be applied either on its own to predict the flow for individual blade sections, such as the mid span of a linear cascade, or in conjunction with a throughflow calculation to predict the performance of a complete axial compressor.

A previous AGARD paper by the author described applications of S1BYL2 to most of the compressor cascade test cases which have subsequently been selected by AGARD Working Group 18: generally good agreement was obtained. This current paper presents new predictions for the V2 and ARL SL19 cascades and for the high speed compressor cases. It is hoped that this will be one of many sets of calculations for these cases, so that an improved understanding of each case may be obtained, together with an appreciation of the strengths and weaknesses of different computational approaches.

LIST OF SYMBOLS

c blade chord
H boundary layer shape factor δ^*/θ
M Mach number
P static pressure
α flow angle, degrees
δ^* boundary layer displacement thickness
θ boundary layer momentum thickness
ω loss coefficient based on upstream conditions
Ω stream tube contraction (upstream/downstream)

Subscripts

1 conditions at upstream boundary of cascade or inlet to blade row

2 conditions at downstream boundary of cascade or exit from blade row

1. INTRODUCTION

Validation/calibration of computer codes against suitable test cases is a highly important area of Computational Fluid Dynamics which is rightly receiving increased attention, as shown for example by Ref 1. The current state-of-the-art for turbomachinery test cases is indicated by the selection made by AGARD Working Group 18 (WG18)[2]. These cover a useful range of practical cascades and rotating machines, and provide a reasonable amount of data on the flow fields as well as measurements of overall performance. However, as noted by WG18 in Chapter III, neither the experimental data nor the flow codes are perfect. Also it is not generally possible to obtain experimental data of many important areas of high speed flows, due primarily to the relatively small scale of turbomachinery blading. Thus some aspects of the codes cannot be adequately validated. Given this situation, there is much to be gained by applying codes to a wide range of test cases and by comparing the results from different codes for the same test cases. An important contribution of WG18 is to have identified a suitable set of test cases to initiate this.

The main code employed in the present work is the RAE S1BYL2 method [3]. This is an inviscid-viscous interaction technique for predicting the blade-to-blade performance of axial compressors. It can be applied either on its own to individual blade sections, such as the mid span of a linear cascade, or linked to a streamline curvature throughflow method in an S1-S2 system to give a complete quasi-three-dimensional prediction of the flow and overall performance of one or more blade rows.

A brief description of the S1BYL2 and S1-S2 methods is given in section 2 of this paper. Section 3 then reviews the results from previous applications [4] of S1BYL2 to the compressor cascade test cases chosen by WG18 and presents further predictions for the V2 high subsonic cascade and new predictions for the ARL SL19 transonic cascade. Results from the RAE S1-S2 system for the three high speed compressor cases are then given in section 4.

2. GENERAL DESCRIPTION OF METHODS

The RAE S1BYL2 method is an inviscid-viscous interaction technique to predict the blade-to-blade performance of axial compressors. The inviscid part consists of a time marching Euler calculation, based on Ref 5, so it can handle transonic flows: shock waves can be captured and the losses due to them can be predicted. The calculation takes place on a specified axisymmetric stream surface, and it includes the effects of rotation and of varying radius and stream tube thickness in the axial direction. The viscous calculation is an integral technique consisting of three parts to estimate laminar boundary layer development, transition point and turbulent boundary layer development respectively. The inviscid-viscous matching procedure employs mixed modes to allow a valid solution to be obtained even when there are regions of separated flow due to shock wave/boundary layer interactions or to excessive diffusion. The viscous calculations continue in the wake downstream of the bladed region, and a compressible flow mixing calculation is carried out on the downstream boundary to determine the mean exit conditions. Thus the method provides both details of the internal flows, including boundary layer development, and predictions of the blade section overall

performance, such as exit flow angle and losses.

In order to employ the S1BYL2 method to predict the performance of complete blade rows, it must be linked with a throughflow calculation which determines the spanwise variations of the flow and ensures that radial equilibrium is satisfied. A semi-automatic S1-S2 procedure for this is described in Ref 6. This procedure has now been automated, with both the S1BYL2 calculation for the blade-to-blade sections and the streamline curvature calculation for the hub-to-tip flow incorporated into one program together with the blade geometry and data link routines. The streamline curvature routine [7] is an improved modular version of that previously employed. It allows curved calculating planes to be specified to give an accurate match to the leading and trailing edges of each blade row. Spanwise mixing terms have been added to some versions of the routine, but these were not included in the present S1-S2 calculations.

The basic principles of the S1-S2 interaction remain the same. Essentially there are three parts to each loop:-

i the performance of the blade-to-blade sections is predicted by S1BYL2 - this involves calculations for up to 9 sections on each blade row.

ii the hub-to-tip flow throughout the whole compressor is calculated by the S2 streamline curvature method, using the pitchwise averaged data from the S1 solutions.

iii the relative flow angles and stream tube geometry from the S1 and S2 parts of the calculation are compared to see whether the solution has converged - if not new blade geometry for each section is found by calculating the intersections between the stream surfaces from the current S2 solution and the blade aerofoils.

Target convergence criteria for the complete S1-S2 solution are typically a) S1 and S2 relative flow angles agreeing to within 0.1°, and b) S1 and S2 stream tube thickness variations agreeing to 0.1%. The number of S1-S2 loops required to achieve this depends on the difficulty of the blade section operating conditions and the number of blade rows involved. About eight loops are generally sufficient for one or two blade rows, but more will be needed, for example, if blade choking is significantly affecting the flow distribution. The solutions from the previous loop provide the starting conditions for calculations on the current loop, so that the procedure is quite efficient. For example, a solution for the HP9 type R0 stage (see section 4.2) requires about 6 hours CPU on a Stardent 1500 mini-supercomputer.

It should be noted that, in order to obtain realistic losses towards the blade ends, empirically derived extra losses must be specified as an input to the S1-S2 system. These additional losses are modelled by a constant drag force in the S1 calculation and the effects are fed to S2 via the normal S1-S2 linking. Although the need for such input is one of the limitations of the S1-S2 approach, the ease with which such corrections can be incorporated in order to tune the model for a given compressor can be a distinct advantage in practice. It is emphasised, however, that apart from the stated end losses and annulus wall blockage factors no other corrections were employed for the cases presented here.

3. COMPRESSOR CASCADE TEST CASES

AGARD Working Group 18 selected four compressor cascades suitable for inviscid-viscous blade-to-blade methods:-

i E/CA-2 V2 High Subsonic Cascade

ii E/CA-3 ONERA 115 High Subsonic Cascade

iii E/CA-4 DFVLR L030-4 Low Supersonic Cascade

iv E/CA-5 ARL SL19 Transonic Cascade

S1BYL2 has previously been applied to the first three of these and the results are given in Ref 4. There was generally good agreement between the test results and predictions, in terms of both internal flow details such as blade surface pressure distributions and overall performance parameters such as static pressure ratio and exit flow angle. The only significant problem area was that increases in losses at high incidence were not predicted directly, but relied on the user noticing the high effective incidence indicated by the solution and specifying revised starting conditions for the surface boundary layer calculation. For cases near optimum incidence, deviation angles were predicted to about ± 1°, static pressure ratios to ± 4% and overall loss coefficients to ± 2% of inlet dynamic head. These levels of accuracy have been confirmed in applications of the code to other cascades, such as the supercritical designs described in Refs 8 and 9.

The test conditions chosen by WG18 for the ONERA 115 and DFVLR L030-4 cascades are the same as, or similar to, those previously studied. Therefore only calculations for the V2 and ARL SL19 cascades will be presented here.

3.1 V2 Subsonic Compressor Cascade

The V2 cascade is a high camber (56.8°), high solidity (2.22) design with 7% thick DCA blade profiles. Twelve test conditions were selected by WG18, covering inlet Mach numbers from 0.3 to 0.85, inlet flow angles from 47.5° to 54.5° and stream tube contraction ratios from 1.08 to 1.39.

As noted in Refs 2 and 4, the axial variation assumed for stream tube thickness between the measured upstream and downstream values is

critical, but also open to uncertainty. Two plausible assumptions could be (a) a linear variation with streamwise distance between the two measuring planes, and (b) constant values upstream and downstream and a linear variation between the leading and trailing edge planes of the cascade. For the V2 cascade, which has a high aspect ratio of 3.75, the former is more likely to be correct and this is confirmed by the calculations for the test condition with values of $M_1/\alpha_1/\Omega$ of 0.80/54.5/1.39 (Fig 1a). Assumption (a) was therefore adopted for all subsequent calculations for this cascade.

The choice of stream tube thickness variation is a good example of a situation where there is uncertainty in the experimental data; and hence where comparisons against other methods run with the same assumptions would be particularly useful.

An 89 x 16 calculating grid was employed for all calculations of the V2 cascade, with 51 x 16 points equally spaced in the axial and tangential directions within the blade row. Outside the row, the axial spacing was increased by a constant factor to give upstream and downstream boundaries for the calculation domain 0.8 axial chords from the blade row.

The twelve WG18 test conditions can be grouped into three categories: (a) choked flow, (b) operation near optimum incidence and (c) stalled flow. The three choked flow conditions are:- 0.85/49.5/1.20, 0.80/47.5/1.17, and 0.80/49.5/1.27. They demonstrate that, relative to a nominal unchoked condition of 0.80/49.5/1.20, choked flow can be produced by small changes in M_1, α_1, or Ω. S1BYL2 successfully predicts this. For example, the predicted Mach number contours, blade surface Mach number distributions and development of the boundary layer displacement thickness and shape factor at 0.85/49.5/1.20 are shown in Fig 1b, together with the test data. There is good agreement between prediction and test, except for the levels of shape factor near the trailing edge of the suction surface.

The point at 0.80/49.5/1.12 is typical of the seven operating conditions near optimum incidence with measured loss coefficients below 5%. The predicted Mach number contours, blade surface Mach number distributions, and boundary layer development are shown in Fig 1c, together with the test data. It can be seen that the overall performance parameters match quite well, although the discrepancy of 1.3° on exit flow angle is higher than usual. There is also close agreement between the predicted inviscid Mach numbers on the blade surfaces and the values deduced from the measured surface static pressures. The agreement between prediction and test for the suction surface boundary layer development is reasonable qualitatively, but the predicted values of shape factor are higher than the test values in the separated flow region near the trailing edge, while the predicted values of displacement thickness near mid chord are lower than the test values. These differences could be due to many reasons. Some of the more obvious ones are:

i errors in the prediction of transition between laminar and turbulent flow

ii the effect of high free-stream turbulence on the turbulent boundary layer - this is not included in the present calculations

iii the general uncertainty in predicting separated turbulent boundary layers

iv errors in measuring very thin boundary layers - the measured displacement thickness is only 0.4 mm at 42% chord

v errors in measuring unsteady flows with a pneumatic probe

vi errors in measuring reverse flows with a forward facing probe

The level of agreement achieved in this case is typical of that for the test conditions near optimum incidence.

The remaining two operating conditions - 0.80/52.5/1.12 and 0.80/54.5/1.23 - are stalled, with measured loss coefficients of over 10%. As previously noted, such conditions can be identified by the fact that maximum blade loading occurs at the leading edge. The user can then specify that the suction surface boundary layer starts as a turbulent layer, with a momentum thickness Reynolds number of about 500. A solution with the boundary layer tripped in this way for the condition 0.80/52.5/1.12 is shown in Fig 1d. The results for surface Mach number and suction surface displacement thickness agree quite well but the predicted shape factors for the suction surface are much higher than deduced from the boundary layer measurements.

In this context it is interesting to consider the loss produced by applying a compressible flow mixing calculation to the measured suction surface boundary layer parameters at 98% chord. At the two stalled flow conditions this loss exceeds the total loss deduced from the wake traverses by about 25%. Assuming that the suction surface loss should be about the same proportion of the total loss as at the other test conditions (ie 80%) implies that the momentum thickness should be about half of the stated value. This would obviously be in much better agreement with the predicted values of momentum thickness and shape factor.

An alternative approach to tripping the boundary layer would be to employ a grid with much closer axial spacing near the leading edge and to assume that all boundary layers are turbulent. This would give solutions broadly comparable with the Navier-Stokes solutions for the V2 cascade shown in Ref 10. However, a grid giving better modelling of the leading edge region would be needed to obtain grid-independent solutions. Also the process of laminar separation, transition and

turbulent reattachment for high incidence flows needs to be understood better so that more realistic models of the viscous flow (either integral boundary layer calculations or turbulence models) can be developed.

3.2 ARL SL19 Transonic Compressor Cascade

The ARL SL19 transonic compressor cascade was derived from a rotor section of a single stage compressor [11] with a design point pressure ratio of 1.9. It is a thin, high stagger (56.9°), low camber(-1.9°) section with a design point inlet Mach number of 1.616. Cascades with similar blades have been tested in facilities at Detroit Diesel Allison (DDA) [12], DFVLR [13] and ONERA [14], and one test point from each series was selected by WG18.

A guide to the relevance of each operating condition can be obtained by computing the pressure ratio and efficiency of a corresponding rotor section from the measured overall cascade performance - for this purpose the rotor section was assumed to have zero inlet absolute flow angle and constant stream surface radius. The results for all the DDA test points taken at the design inlet Mach number [12] were as follows:-

Cascade static pressure ratio	Rotor total pressure ratio	Rotor adiabatic efficiency %
1.220	1.086	67.8
1.468	1.180	77.0
1.672	1.318	81.8
1.870	1.489	84.0
2.036	1.674	84.8
2.097	1.727	83.8
2.220	1.801	81.1
2.300	1.868	82.2

This clearly shows that the points with higher static pressure ratios are of greater practical interest to the compressor engineer, and it is these which the S1BYL2 method was developed to predict. Of the WG18 test conditions only the DFVLR point falls into this category.

For the S1BYL2 calculation of the DFVLR test point the stream tube thickness was assumed to be constant upstream of the cascade leading edge and to reduce linearly with axial distance to the measured value at the traverse plane 47% of gap axially downstream of the blade trailing edge. A 119 x 21 calculating grid was employed for the time marching part of the calculation, with 81 x 21 points within the blade row equally spaced in both axial and tangential directions. The test value of inlet tangential velocity was specified and the operating condition for the solution was chosen such that the main pressure rise on the suction surface occurred close to the measured position.

The predicted Mach number contours, blade surface Mach number distributions and boundary layer development for the design blade shape are shown in Fig 2, together with the Mach numbers deduced from the measured surface static pressures and the predicted inviscid total pressures. The agreement between prediction and test is generally good. Note that the calculation indicates the presence of strong shock wave/boundary layer interactions on both the suction and pressure surfaces of the blade. It is possible that the pre-shock boundary layer on the pressure surface could be laminar, although transition has been forced upstream of the shock in the S1BYL2 solution, and this might explain the discrepancies between prediction and test in this region. The agreement between measured and predicted overall performance parameters is reasonable - the predicted unique incidence inlet angle and the exit flow angle are both 1° too high, static pressure rise agrees to about 5%, and total pressure loss is 10% compared with a measured value of 12%.

The predictions are quite sensitive to the assumptions made about stream tube thickness. For example, taking a constant value upstream of the initial shock wave reduces the predicted inlet flow angle by 0.8°, while assuming a linear variation between the plane of the upstream static pressure tappings and the downstream traverse plane increases the value by 0.8°. There is also some uncertainty about the appropriate blade shape to use for the calculations, since the two instrumented blades in the cascade both differed slightly from the design intent and some blade deformation due to the aerodynamic loads was observed during testing [15]. Using the measured shape of the suction surface blade given in Ref 2 reduces the predicted inlet flow angle by 0.7°, whereas the shape for the pressure surface blade is much closer to the design intent.

Once again calculations with a number of different codes would be instructive and might enable a consensus view to be reached of the appropriate boundary conditions to be applied.

4. HIGH SPEED COMPRESSOR TEST CASES

As mentioned above, the S1-S2 system incorporating S1BYL2 has been applied to all three high speed compressor test cases selected by WG18 viz:

i E/CC-2 NASA Transonic Rotor 67

ii E/CO-3 RR HP9 Subsonic Stage

iii E/CO-4 DFVLR Transonic Stage

The system was kept the same throughout and similar calculating grids were applied. Nine S1 sections were used to model each blade row and the grids used for the time marching part of the S1BYL2 calculations were similar to those used for the cascades in section 3 above. The S2 solutions typically employed 21 streamlines and there were 4 interblade calculating planes between the leading and trailing edge planes of each blade row.

The inlet total pressure profiles for each compressor were based closely on the measured data, except that no attempt was made to

achieve zero values of velocity at the walls. Small amounts of annulus wall blockage, about 1% for the two transonic fans and 2½% for HP9, were included to allow for this. The losses used to model end effects were assumed to affect the outer regions of each row: the loss coefficients were specified to drop from 15% at the annulus walls, to zero at a distance of 1/3 rotor chord from the walls. This assumption is in line with that made for previous S1-S2 calculations of the rotor row of transonic civil fans[6,16]. If more than one stage were being considered, it would obviously be necessary either to include the effect of spanwise mixing within the S2 part of the calculation, or to use a more even distribution of extra loss.

4.1 NASA Transonic Rotor 67

Rotor 67 is the first stage rotor of a two stage fan. It was tested as an isolated row to provide data for comparison with numerical predictions which were free from circumferential variations due to stationary blade rows. The rotor has an aspect ratio of 1.6 based on average span/mid height chord, and at inlet the tip diameter is 514 mm with a hub/tip ratio of 0.375. The design point conditions are a tip speed of 429 m/s, an inlet tip relative Mach number of 1.38, a rotor pressure ratio of 1.63 and a mass flow rate of 33.25 kg/s. Laser anemometry was extensively used to measure details of the internal flow fields, and radial traverses with a combination probe were carried out to determine the inlet and exit variations of total and static pressure, total temperature and flow angle.

Two operating conditions were selected by WG18 - one near peak efficiency and the other near stall. The flow at both conditions was predicted using the S1-S2 system and some of the results are shown in Figs 3 and 4. Considering firstly the overall performance, the mass flow rate at the pressure ratio for the peak efficiency condition was predicted to be 34.0 kg/s, about 1½% below the test value. Predicted adiabatic efficiency was 92.3%, compared with a test value of 93%. At the mass flow for the near stall point, the predicted pressure ratio and efficiency were 1.727 and 91.6%, compared with test values of 1.728 and 90.1%. There is also good agreement between the predicted and measured radial profiles of total pressure and temperature at rotor exit, as shown in Fig 3. (The values plotted are relative to the inlet conditions at mid span.)

The predicted Mach number contours at the two conditions for the blade-to-blade sections at 30%, 70% and 90% span from the hub are shown in Fig 4, together with the predicted blade surface Mach numbers and boundary layer development. The contours may be compared directly with the corresponding plots deduced from the test data given in Fig 17 of Ref 2. The agreement is quite good for the outer sections, with the S1-S2 system correctly predicting the dual shock system noted in Ref 17 at the peak efficiency condition, and the single normal shock wave just detached from the blading at the near stall condition.

However, the calculation predicts a more distinct shock in the uncovered passage at 30% blade height for both conditions than was measured with the laser anemometer.

The predicted boundary layer development for the suction surface indicates a trailing edge separation for the sections over the inner third of the span, with the shock wave/boundary layer interaction near mid chord becoming significant and causing some separation over the outer half of the blade. The interaction is sufficiently strong at the peak efficiency condition to cause complete separation of the boundary layer downstream of the shock for the tip sections.

4.2 RR HP9 Subsonic Compressor Stage

The Rolls-Royce HP9 rig is a single stage model of one of the later stages in a civil HP compressor. It therefore has a much higher inlet hub/tip ratio (0.84) and lower rotor aspect ratio (0.9) than the other two WG18 compressor cases. Inlet spoiler rings are employed to generate a suitable inlet velocity profile. The type "RD" case selected by WG18 has conventional blade profiles, a design stage pressure ratio of 1.24, a mass flow rate of 9.1 kg/s and a tip speed of 251.3 m/s at ISA inlet conditions. Tip diameter is 518.2 mm.

All three operating conditions - maximum flow, mid chic and near surge - were studied using the S1-S2 system. The predictions at maximum flow and mid chic were straightforward, but the initial attempts for the near surge point failed. The high incidences for the S1 sections nearest the hub caused very high levels of profile loss to be predicted for this region: these resulted in even more arduous flow conditions being calculated for the next S1-S2 loop by the S2 part of the system and eventually the S1BYL2 calculations failed to converge. The present S1-S2 technique is probably over-sensitive to local flow problems like this, since there is no allowance for spanwise movement of low energy boundary layer flows - inclusion of spanwise mixing in the S2 calculation should help in this respect. Also, the assumption that stream surfaces remain axisymmetric means that the relief of the endwall flow conditions due to three-dimensional flows is neglected, a fundamental limitation of the axisymmetric S1-S2 approach. To enable a solution to be obtained for HP9 at the near surge mass flow, S1 calculations were carried out only between 10% and 90% blade heights (the other S1-S2 solutions included calculations for sections within 5% height of the walls) with extrapolation used to obtain the conditions for stream surfaces closer to the walls.

Predicted Mach number contours and distributions and boundary layer development for the rotor and stator mid height sections at the three operating conditions are shown in Fig 5. These demonstrate the range of operating incidences which are to be expected at different points along a constant speed characteristic for a single stage compressor - high positive blade loadings at the leading edge

near surge, roughly zero loading at mid chic and high negative loadings at maximum flow. The predicted boundary layer behaviour is typical of blade sections with circular arc camber lines. On the suction surface the shape factors are relatively low over most of the chord, indicating attached boundary layers. However, there is rapid growth near the trailing edge where the boundary layer has become too thick to withstand the constant diffusion associated with the circular arc camber line and separates. On the pressure surface the boundary layer remains attached throughout, apart from a possible laminar bubble near the leading edge at the maximum flow point. No interblade measurements are available for comparison with these data.

There is some uncertainty about the rotor exit conditions for this case [2], and so the comparisions shown between prediction and test (Fig 6) are for the circumferentially averaged conditions downstream of the stator. The main discrepancies are that:-

i the temperature rises near the outer casing are overestimated - this could be due to the relatively crude allowance for end wall effects, or to neglecting spanwise mixing effects in the S2 throughflow calculation.

ii the predicted efficiencies at the near surge condition are much higher than measured - this is probably associated with the problems in predicting high incidence flows noted in section 3.1 above. Improved agreement could be obtained by "tripping" the suction surface boundary layers at the blade leading edge.

Apart from this the agreement obtained is reasonable, particularly when the uncertainty due to the manufacturing tolerance of 0.75° on blade stagger angle is considered. If the prediction at the maximum flow point is repeated with the rotor and stator rows restaggered open by this amount, then at the same exit flow function there are increases of 0.9% on mass flow, 0.012 on pressure ratio and 1.2% on efficiency.

4.3 DFVLR Transonic Compressor Stage

The DFVLR transonic fan has an inlet tip diameter of 398 mm, an inlet hub/tip ratio of 0.5 and a rotor aspect ratio of 1.7. The design point pressure ratio is 1.51 at a mass flow rate of 17.3 kg/s and a blade tip speed of 421 m/s. The rotor has been tested with two different stator rows: the laser anemometry measurements of the rotor flow field were taken with the NACA 65/60 stator row and this is the configuration which has been studied using the S1-S2 system.

Predictions were carried out at the same exit mass flow functions as the two test conditions selected by WG18 and the predicted and measured radial distributions of performance are compared in Fig 7. The agreement is much poorer than for the other two compressors The main problem seems to be that the S1-S2 system over-estimates the rotor efficiency by about 4% at both conditions, and this results in significantly higher pressure ratios being predicted at a given mass flow. The magnitude of this discrepancy is disappointing, given the level of agreement on overall performance for the other two cases and for other transonic fans. In particular the S1-S2 system has not identified any reason for the peak efficiency of the DFVLR rotor being over 5% lower than for NASA rotor 67, which has a similar pressure ratio, tip speed and aspect ratio. It will be interesting to see whether other CFD methods can explain this difference.

Despite the poor agreement on overall performance, the predicted Mach number contours for the rotor at 18%, 45%, 68% and 89% blade heights are in close agreement with those given in Figs 10 and 11 of Ref 2 (See Fig 8). At peak efficiency the solution correctly predicts an oblique leading edge shock near the rotor tip with a maximum suction surface Mach number of about 1.4. At 68% height the shock is becoming more normal, and by 45% height it is detached from the blade leading edge. The predicted diffusion of the flow within the blade passage also matches the test data well. The predicted suction surface boundary layer development shows a gradual progression with blade height, roughly similar to that for NASA rotor 67. Near the hub, separation occurs only near the trailing edge; by about 45% height the shock wave/boundary layer interaction has become strong enough to cause a small separation bubble at about mid chord, and the extent of the separation at the trailing edge has reduced; at 68% height the mid chord separation has increased and the trailing edge separation has disappeared; and at 89% the shock wave/boundary layer interaction is strong enough to cause complete separation for the rear part of the blade.

At the point nearer surge, the shock wave has moved forward and it is just detached from the leading edge at 89% height in both predicted and measured results. The shock becomes further detached at 68% and 45% heights, and at 18% there is only a small region near the leading edge where the flow is supersonic. The predicted boundary layer behaviour is similar to that at peak efficiency except that the shock/boundary layer interaction near the tip is predicted to be slightly weaker and the boundary layer reattaches before the trailing edge. However, given the high effective incidences indicated over the inner half of the blade, it is likely that the actual suction surface boundary layers are rather thicker.

5. CONCLUDING REMARKS

The S1BYL2 inviscid-viscous interaction method has now been applied to all the high speed compressor cascade test cases selected by AGARD WG18, and, linked with a streamline curvature throughflow method in an S1-S2 system, to all the high speed compressor cases. The predictions obtained are generally in encouraging agreement with the experimental data, both in terms of the

features of the internal flows and the overall performance parameters.

For the compressor cascades the blade choking/unique incidence angles and deviation angles are predicted to about ± 1°, the static pressure rise to ± 4% and (less satisfactorily) the total loss coefficient to ± 2% of inlet dynamic lead, for operation below stalling incidence. The increased losses which occur at high positive incidence are not fully predicted automatically, but such situations can be detected by examining the effective incidence predicted for the blade. It is believed that improvements are needed both in the viscous modelling and in the numerical resolution of the leading edge region before this type of flow can be predicted correctly.

For the compressor test cases, the predicted results for the NASA rotor 67 and for the HP9 stage agree well with the measured results. In particular, peak efficiency levels are estimated to within about 1%. The results for the DFVLR stage are less satisfactory: the rotor efficiency is over-estimated by about 4%, despite close agreement between the measured and predicted blade-to-blade Mach numbers. Thus the present method fails to explain the difference of over 5% in measured rotor efficiency between the NASA 67 and DFVLR rotors. It will be interesting to see whether other methods are more successful.

The present applications of the RAE S1BYL2 code to the WG18 compressor test cases have been valuable, both in evaluating the code and in gaining further understanding of the test cases. The author would like to congratulate the Working Group for taking the lead in identifiying this set of cases, and he would encourage others to carry out and publish corresponding predictions.

REFERENCES

1. "Validation of Computational Fluid Dynamics", AGARD CP 437, May 1988.

2. "Test Cases for Computation of Internal Flows in Aero Engine Components", AGARD AR275, July 1990.

3. Calvert, W. J., "An inviscid-viscous interaction treatment to predict the blade-to-blade performance of axial compressors with leading edge normal shock waves", ASME Paper 82-GT-135, 1982.

4. Calvert, W. J., "Application of an inviscid-viscous interaction method to transonic compressor cascades", in "Viscous Effects in Turbomachines", AGARD CP 351, June 1983, paper 2.

5. Denton, J. D., "An improved time marching method for turbomachinery flow calculation", ASME Journal of Eng for Power, Vol 105, pp 514-524, 1983.

6. Calvert, W. J., and Ginder, R. B., "A quasi-three-dimensional calculation system for the flow within transonic compressor blade rows", ASME Paper 85-GT-22, 1985.

7. Dunham, J., et al, "A new turbomachinery throughflow program using the streamline curvature method", Unpublished RAE report, 1990.

8. Fuchs, R., et al, "Experimental investigation of a supercritical compressor rotor blade section", in "Advanced Technology for Aero Gas Turbine Components", AGARD CP 421, May 1987, Paper 39.

9. Steinert, W., et al, "Design and testing of a controlled diffusion airfoil cascade for industrial axial flow compressor application", ASME Paper 90-GT-140, 1990.

10. Dawes, W. N., "A comparison of zero and one equation turbulence modelling for turbomachinery calculations", ASME Paper 90-GT-303, 1990.

11. Wennerstrom, A. J., "Experimental study of a high-through-flow transonic axial compressor stage", Proceedings 6th ISABE, Paris, pp 447-457, 1983.

12. Fleeter, S., et al, "Experimental investigation of a supersonic compressor cascade", ARL TR 75-0208, June 1975.

13. Tweedt, D. L., et al, "Experimental investigation of the performance of a supersonic compressor cascade", ASME Paper 88-GT-306, 1988.

14. Fourmaux, A., et al, "Test results and theoretical investigations on the ARL 19 supersonic blade cascade", ASME Paper 88-GT-202, 1988.

15. Schreiber, H. A., and Tweedt, D. L., "Experimental investigation and analysis of the supersonic compressor cascade ARL-2DPC", DFVLR IB-325-02-87, 1987.

16. Calvert, W. J., et al, "Performance of a civil fan rotor designed using a quasi-three-dimensional calculation system", in "Turbomachinery - Efficiency Prediction and Improvement", Proc I Mech E, 1987-6,

17. Pierzga, M. J., and Wood, J. R., "Investigation of the three-dimensional flow field within a transonic fan rotor: experiment and analysis", ASME Journal of Eng for Gas Turbines and Power, Vol 107, No 2, April 1985, pp 436-449.

18. Wadia, A. R., and Beacher, B. F., "Three-dimensional relief in turbomachinery blading", ASME Journal of Turbomachinery, Vol 112, No 3, pp 587-598, 1990.

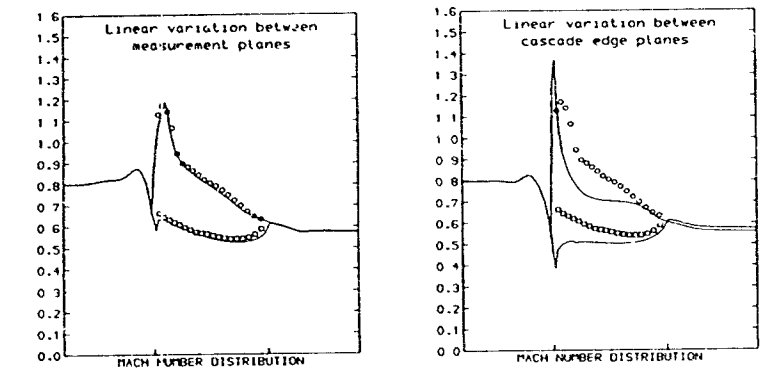

a. Effect of stream tube thickness at M1=0.8, AL1=54.5, Omega=1.39

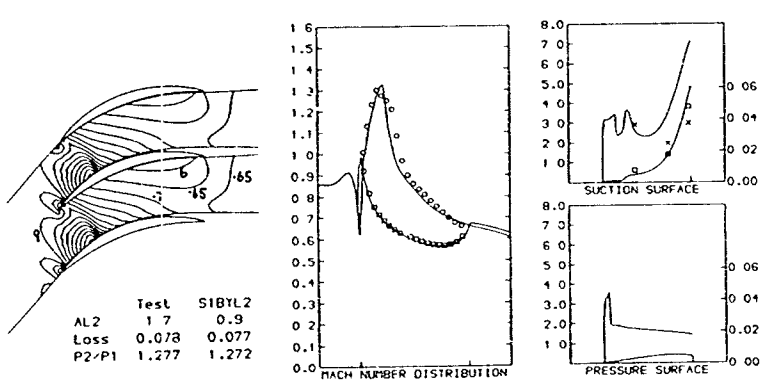

b. Choked flow case - M1=0.85, AL1=49.5, Omega=1.20

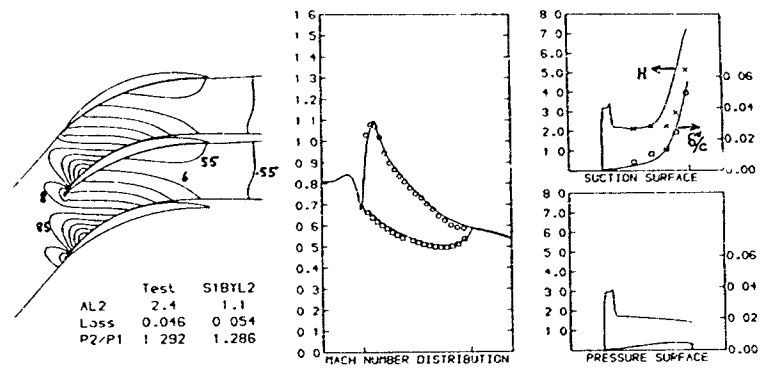

c. Optimum incidence case - M1=0.8, AL1=49.5, Omega=1.12

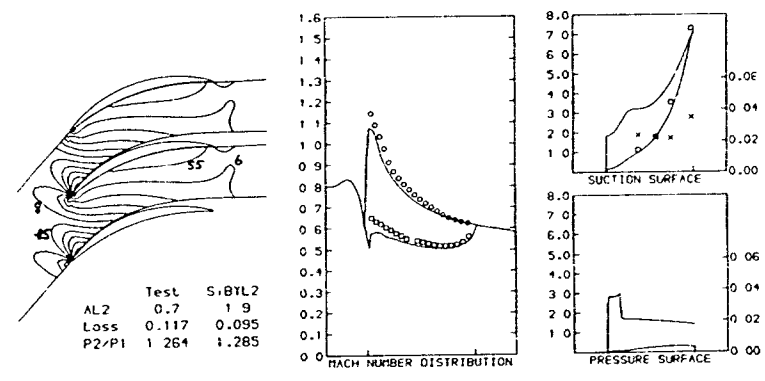

d. Stalled flow case - M1=0.8, AL1=52.5, Omega=1.12

Fig 1 SIBYL2 predictions for V2 cascade (symbols indicate test data)

Figs 2&3

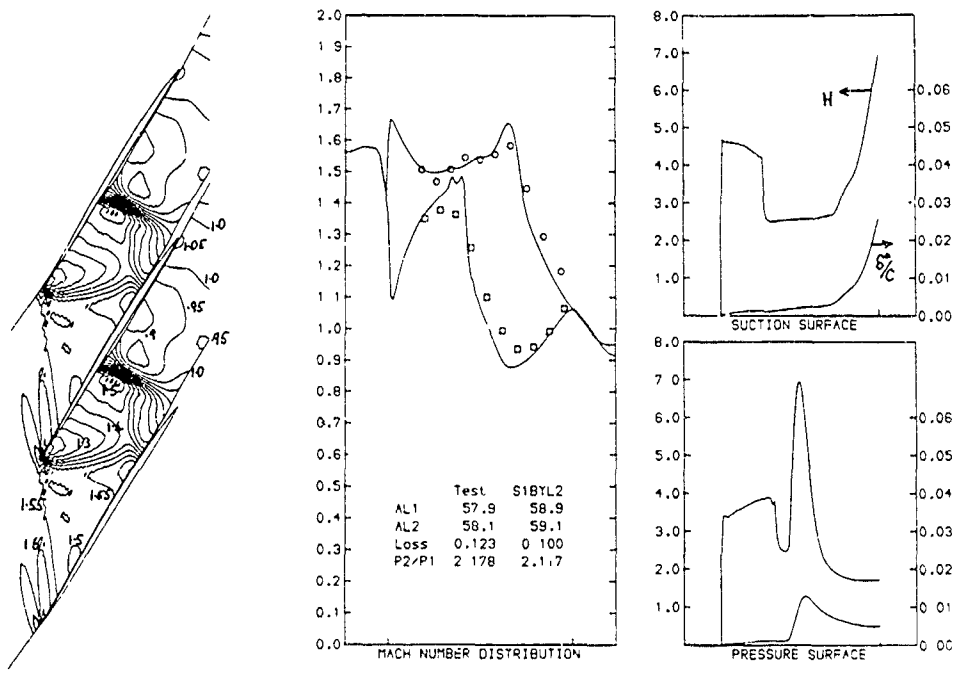

Fig 2 S1BYL2 prediction for ARL SL19 cascade (symbols indicate test data)

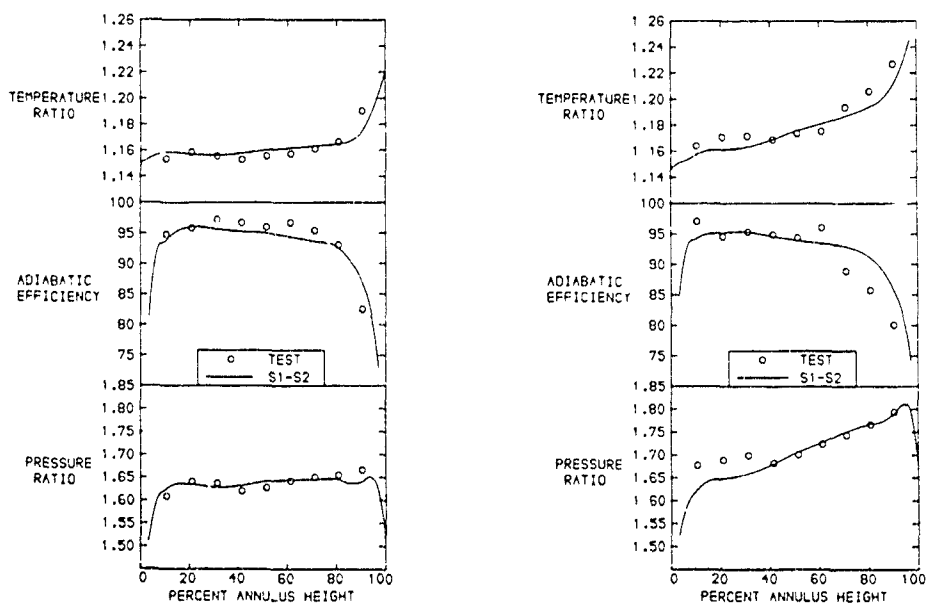

a. Radial profiles near peak efficiency

b. Radial profiles near stall

Fig 3 S1-S2 predictions for NASA transonic rotor 67

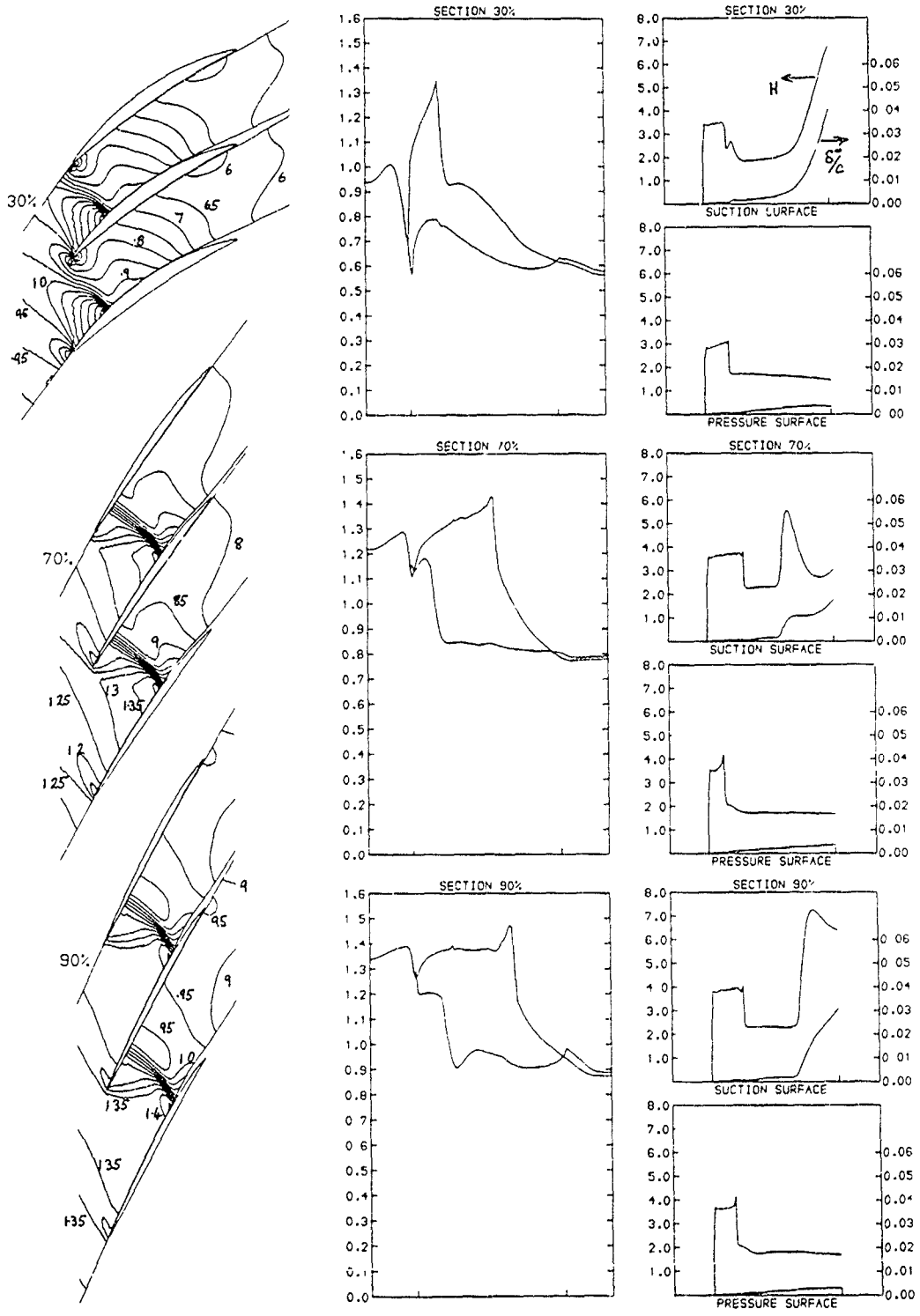

Fig 4a SIBY.2 predictions for NASA rotor 67 at peak efficiency

TMP 1204

Fig 4b

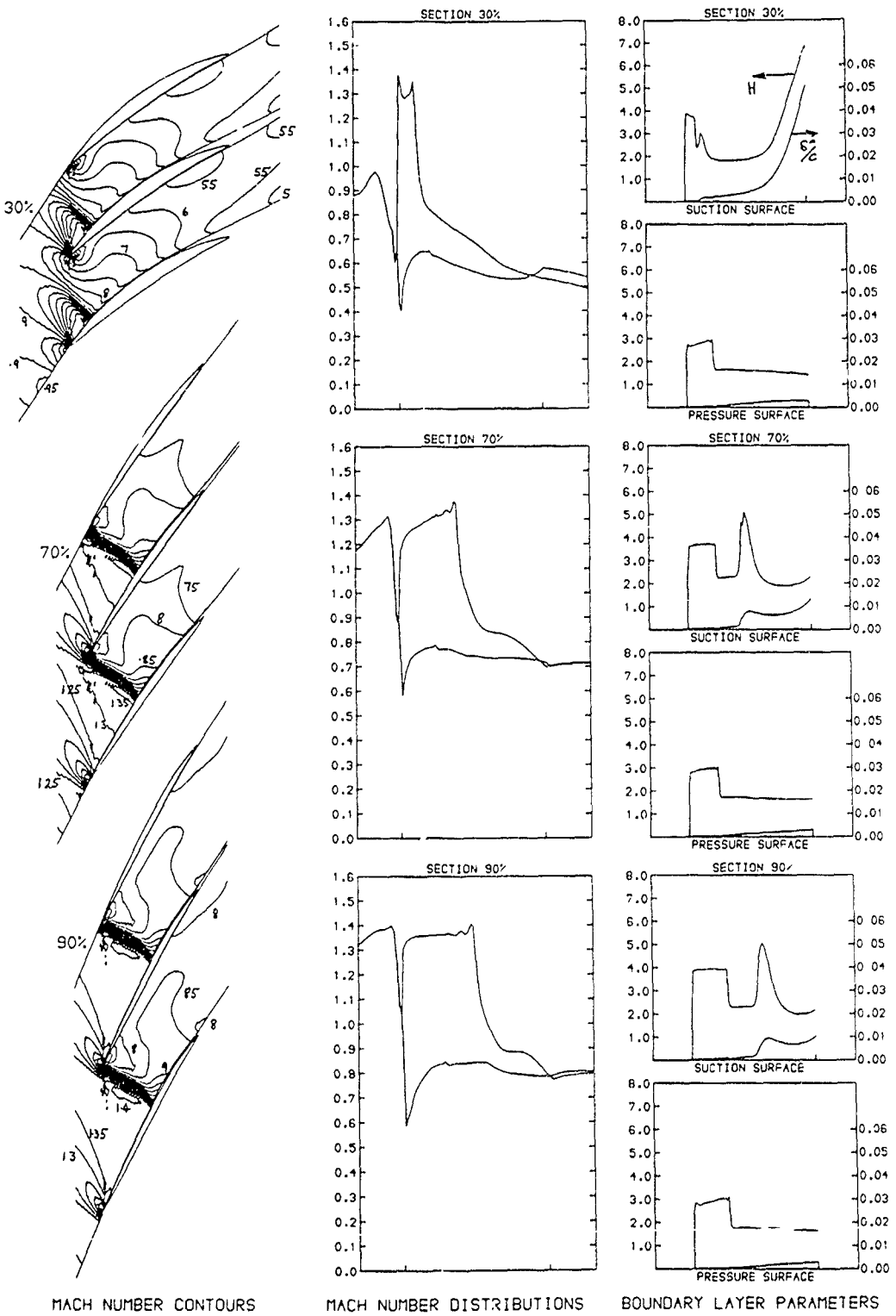

Fig 4b S1BYL2 predictions For NASA rotor 67 near stall

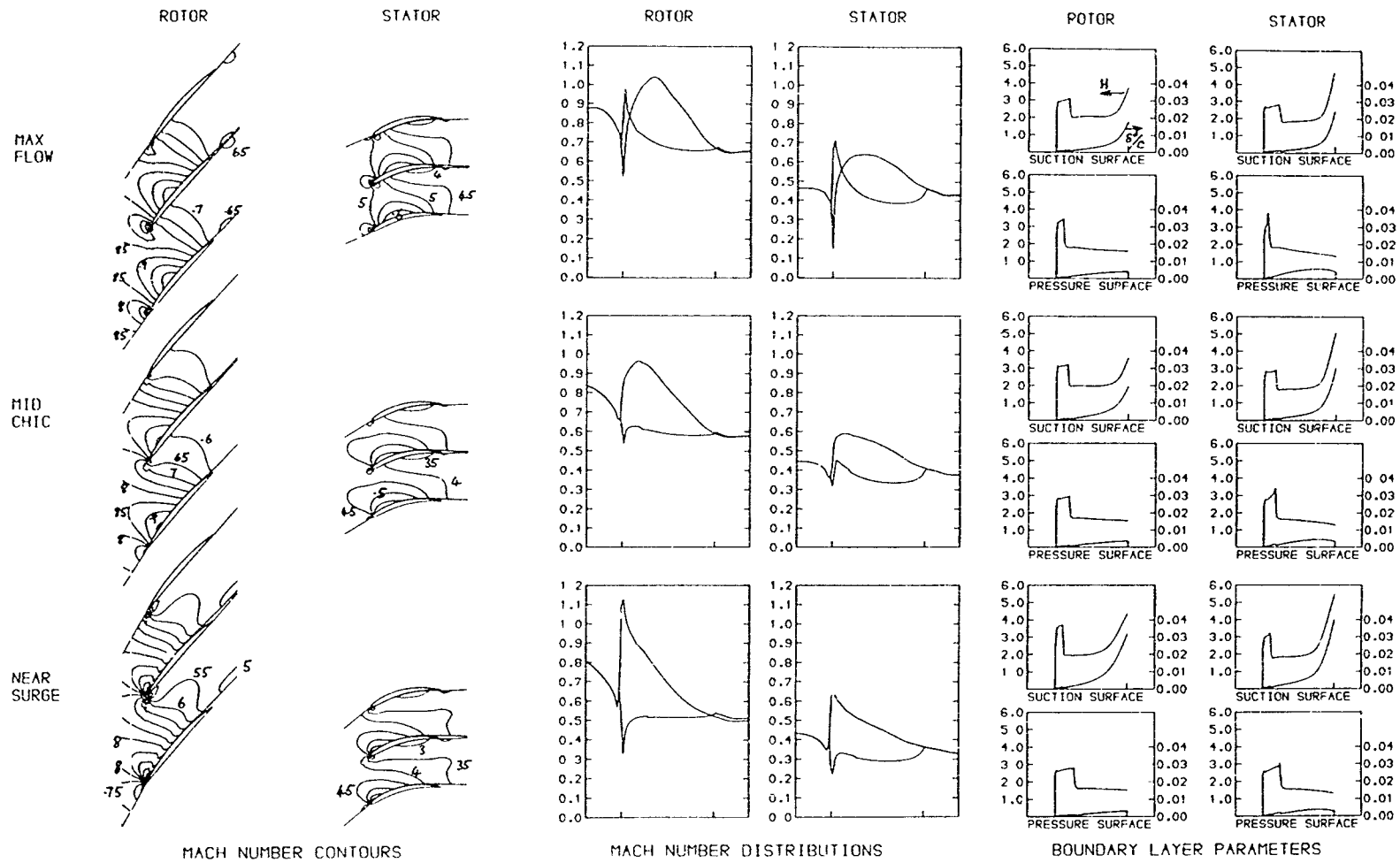

Fig 5 S1BYL2 predictions for Rolls-Royce HP9 mid span sections

Figs 6&7

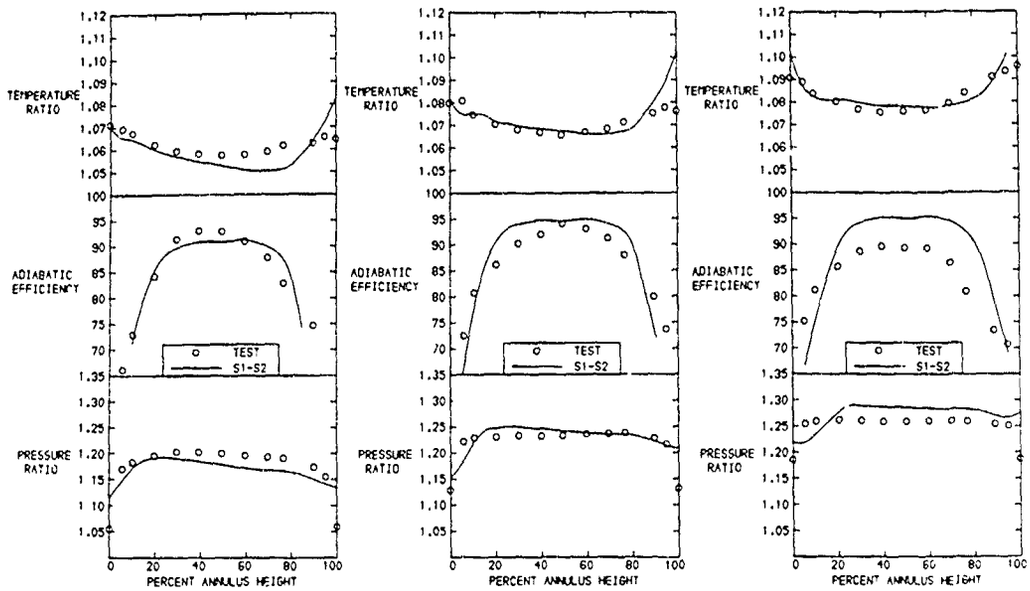

a. Radial profiles at max flow b. Radial profiles at mid chic c. Radial profiles near surge

Fig 6 S1-S2 predictions for Rolls-Royce HP9 stage

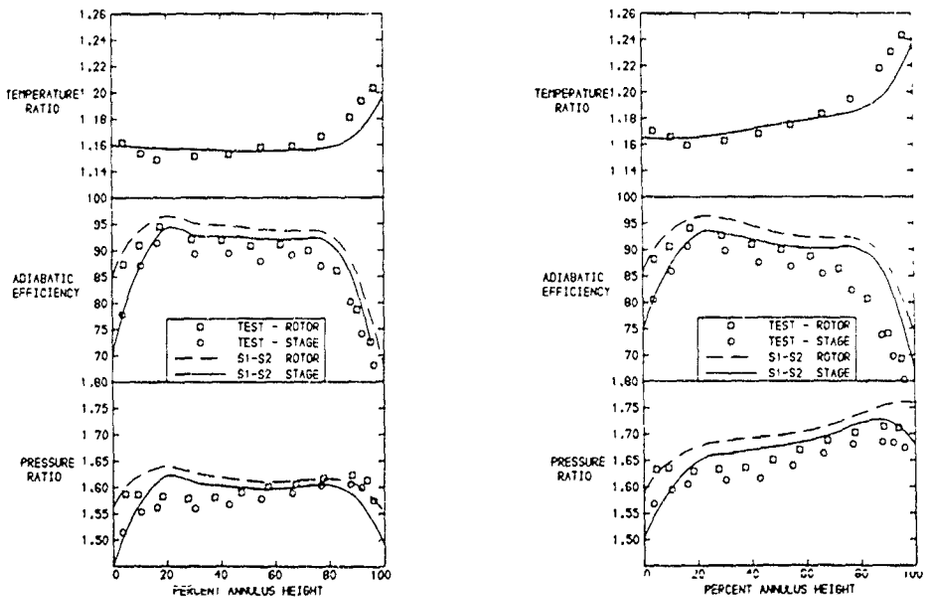

a. Radial profiles near peak efficiency b. Radial profiles near stall

Fig 7 S1-S2 predictions for DFVLR transonic stage

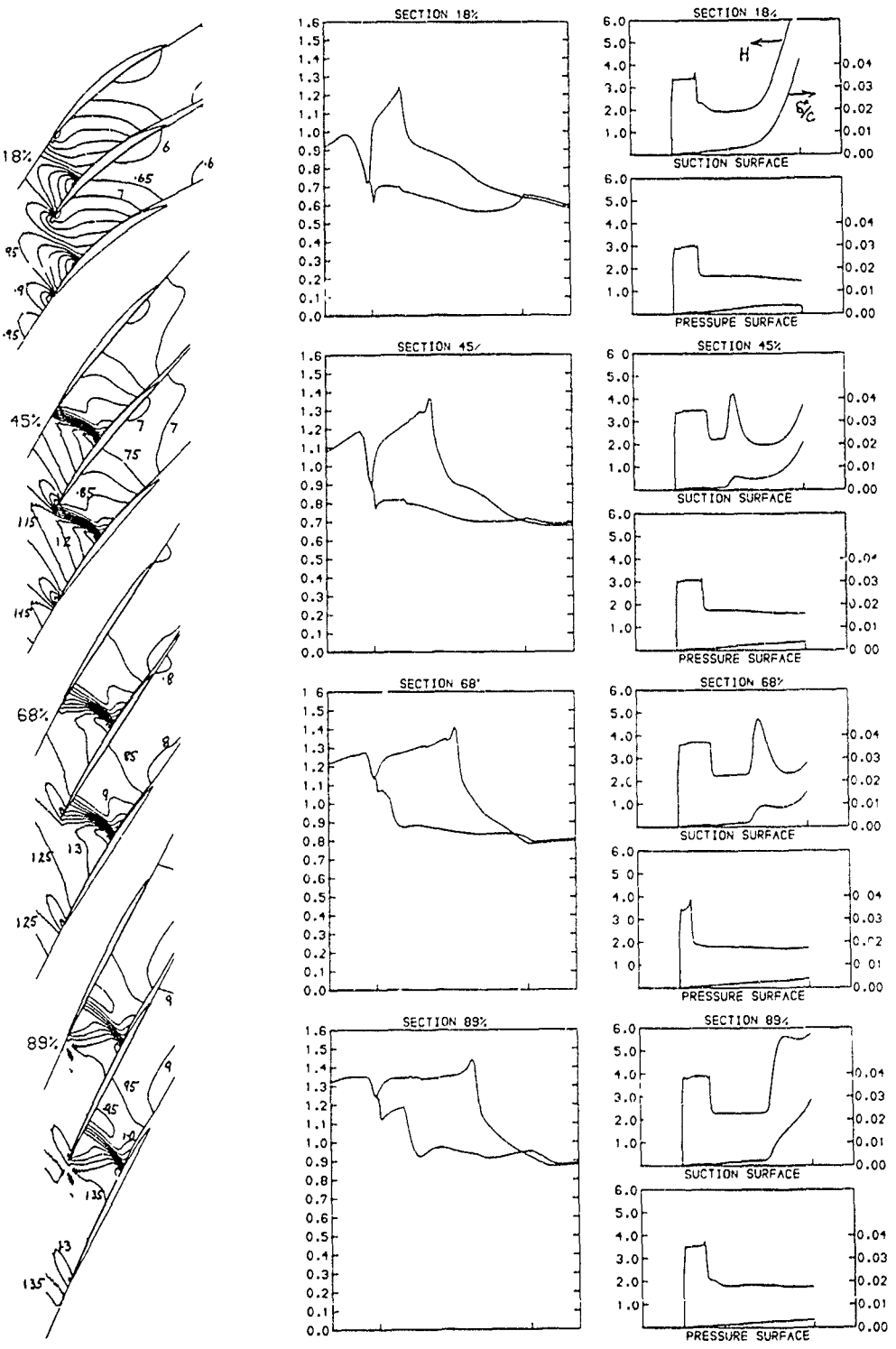

Fig 8a S1BYL2 predictions for DFVLR rotor at peak efficiency

Fig 8b

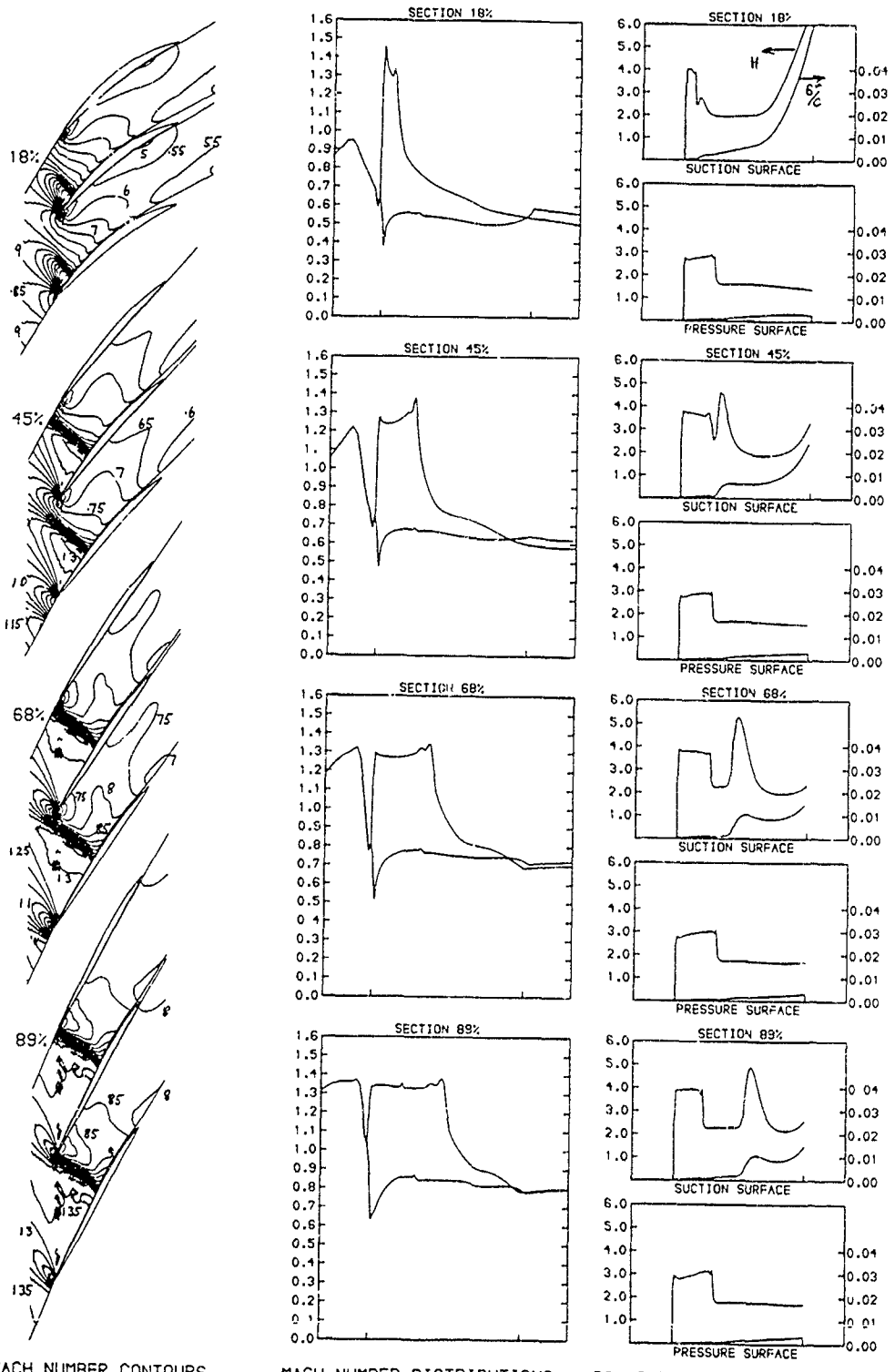

Fig 8b S1BYL2 predictions for DFVLR rotor near surge

REPORT DOCUMENTATION PAGE

Overall security classification of this page

UNLIMITED

As far as possible this page should contain only unclassified information. If it is necessary to enter classified information, the box above must be marked to indicate the classification, e.g. Restricted, Confidential or Secret.

1 DRIC Reference (to be added by DRIC)	2. Originator's Reference	3. Agency Reference	4. Report Security Classification/Marking
	RAE TM P 1204		UNLIMITED

5 DRIC Code for Originator	6. Originator (Corporate Author) Name and Location
7674300E	Royal Aerospace Establishment, Pyestock, Hants, UK
5a Sponsoring Agency's Code	6a. Sponsoring Agency (Contract Authority) Name and Location
N/A	N/A

7 Title Application of SIBYL2 to the AGARD WG18 compressor test cases

7a (For Translations) Title in Foreign Language

7b. (For Conference Papers) Title, Place and Date of Conference

77th Symposium of the AGARD Propulsion and Energetics Panel on "CFD Techniques for Propulsion Applications", to be held in San Antonio, Texas, USA, 27-31 May 1991

8 Author 1. Surname, Initials	9a. Author 2	9b. Authors 3, 4	10. Date	Pages	Refs
Calvert, W.J.			February 1991	17	18

11 Contract Number	12. Period	13. Project	14. Other Reference Nos.

15. Distribution statement

(a) Controlled by –

(b) Special limitations (if any) –

If it is intended that a copy of this document shall be released overseas refer to RAE Leaflet No.3 to Supplement 6 of MOD Manual 4.

16 Descriptors (Keywords) (Descriptors marked * are selected from TEST)

Axial flow compressors*. Compressor blades*. Turbomachinery*. SIBYL2. Cascades. Test cases.

17. Abstract

SIBYL2 is an inviscid-viscous blade-to-blade method for calculating the detailed aerodynamics and overall performance of compressor blades. It may be applied either on its own to predict the flow for individual blade sections, such as the mid span of a linear cascade, or in conjunction with a throughflow calculation to predict the performance of a complete axial compressor.

A previous AGARD paper by the author described applications of SIBYL2 to most of the compressor cascade test cases which have subsequently been selected by AGARD Working Group 18: generally good agreement was obtained. This current paper presents new predictions for the V2 and ARL SL19 cascades and for the high speed compressor cases. It is hoped that this will be one of many sets of calculations for these cases, so that an improved understanding of each case may be obtained, together with an appreciation of the strengths and weaknesses of different computational approaches.

F5910/1